Silver Nanoparticles and Chitosan Oligomers Composites as Poplar Wood Protective Treatments against Wood-Decay Fungi and Termites

Eleana Spavento [1], María Teresa de Troya-Franco [2], Luis Acuña-Rello [3], Mónica Murace [1], Sara M. Santos [2], Milagros Casado-Sanz [3], Roberto D. Martínez-López [3], Jesús Martín-Gil [4], Javier Álvarez-Martínez [4] and Pablo Martín-Ramos [4,*]

1   Wood Research Laboratory (LIMAD), School of Agrarian and Forestry Sciences, National University of La Plata, Diag. 113 N° 469, La Plata B1904, Argentina; eleana.spavento@agro.unlp.edu.ar (E.S.); monica.murace@agro.unlp.edu.ar (M.M.)
2   Institute of Forest Sciences (ICIFOR) and Crop Protection Department, National Institute of Agrarian and Food Research and Technology (INIA)—Superior Council for Scientific Research (CSIC), Ctra. Coruña km. 7, 28040 Madrid, Spain; troya@inia.csic.es (M.T.d.T.-F.); santos@inia.csic.es (S.M.S.)
3   Timber Structures and Wood Technology Research Group, Department of Agricultural and Forestry Engineering, ETSIIAA, University of Valladolid, Avda. Madrid 44, 34004 Palencia, Spain; maderas@iaf.uva.es (L.A.-R.); mmcasado@uva.es (M.C.-S.); robertodiego.martinez@uva.es (R.D.M.-L.)
4   Advanced Materials Laboratory, Department of Agricultural and Forestry Engineering, ETSIIAA, University of Valladolid, Avda. Madrid 44, 34004 Palencia, Spain; jesus.martin.gil@uva.es (J.M.-G.); javier.alvarez.martinez@uva.es (J.Á.-M.)
*   Correspondence: pmr@uva.es

Abstract: This study focuses on *Populus ×euramericana* (Dode) Guinier, a globally distributed fast-growing tree. Despite its valuable wood, it exhibits low durability. The aim of this study was to assess the efficacy of a binary composite comprising silver nanoparticles (AgNPs) and chitosan oligomers (COS) in protecting *P. ×euramericana* 'I-214' wood against degradation caused by xylophagous fungi and termites through vacuum-pressure impregnation. The test material was carefully selected and conditioned following the guidelines of EN 350:2016, and impregnation was carried out in accordance with EN 113-1:2021. Five concentrations of AgNPs–COS composites were utilized. Biodeterioration resistance was evaluated based on EN 350:2016 for white (*Trametes versicolor* (L.) Lloyd) and brown (*Coniophora puteana* (Schumach.) P.Karst.) rot fungi, and EN 117:2012 for subterranean termites (*Reticulitermis grassei* Clément). The durability class and use class were assigned following EN 350:2016 and EN 335:2013, respectively. In comparison to the untreated control, the binary solution at its highest concentration (AgNPs 4 ppm + COS 20 g·L^{-1}) demonstrated a notable reduction in weight loss, decreasing from $41.96 \pm 4.49\%$ to $30.15 \pm 3.08\%$ for white-rot fungi and from $41.93 \pm 4.33\%$ to $27.22 \pm 0.66\%$ for brown rot fungi. Furthermore, the observed termite infestation shifted from "heavy" to "attempted attack", resulting in a decrease in the survival rate from $53.98 \pm 10.40\%$ to $26.62 \pm 8.63\%$. Consequently, the durability classification of *P. ×euramericana* I-214 witnessed an enhancement from "Not durable" to "Slightly" and "Moderately durable" concerning decay fungi and termites, respectively. These findings expand the potential applications of this wood and substantiate the advantages of employing this environmentally friendly treatment.

Keywords: AgNPs; *Coniophora puteana*; durability; nanocomposite; pressure-vacuum treatment; *Populus ×euramericana*; *Reticulitermes grassei*; *Trametes versicolor*; use class

1. Introduction

The inherent resistance of wood to decay induced by fungi, termites and other insects, and marine borers, as defined in EN 350:2016 [1], establishes its natural durability. This property enables the identification of the optimal utilization scenario for wood or

the specification of the necessary protective measures corresponding to its anticipated utilization class.

Xylophagous fungi, responsible for brown and white rot, along with subterranean termites, stand out as the most aggressive agents causing damage to wood in service. These fungi induce structural alterations, impacting the inherent resistance of wood through enzymatic attacks on the polymeric fraction of the cell wall, encompassing cellulose, hemi-celluloses, and lignin. In turn, termites contribute to the structural weakening of wood through a dual process of mechanical chewing and enzymatic digestion of lignocellulosic components. This enzymatic digestion is facilitated by symbiotic microorganisms residing in their digestive tract [2–4].

Populus ×euramericana (Dode) Guinier (=*Populus ×canadensis* Moench; poplar) clone 'I-214' holds significant representativeness and economic importance in Spain [5]. Nevertheless, the inherent low natural durability of its wood constrains its potential applications and usage scenarios [6]. Thus, there is a need to develop treatments aimed at enhancing its resistance to deterioration.

The application of preservative substances to wood through vacuum-pressure treatment has long been recognized as an effective strategy for enhancing wood durability. However, numerous chemical compounds commonly employed for this purpose exhibit limitations, particularly in terms of environmental sustainability and human health considerations. Consequently, there is a critical need to explore innovative technologies and alternative preservatives, diverging from those traditionally utilized, to broaden the spectrum of wood applications and extend its useful life, especially in scenarios where natural durability may not be sufficient.

In the realm of wood enhancement, nanotechnology is emerging as a transformative force, focusing on improving the properties of wood and wood products, particularly in terms of dimensional stability and resistance to microorganism attacks. This advancement involves the impregnation or coating of wood, with its standout feature being its capability to deeply infiltrate the wood substrate, facilitated by its minute size (smaller than the voids in the wood cell wall). This penetration allows nanotechnology to effectively modify the surface chemistry, yielding a more potent and enduring impact [7–9].

Recent investigations have delved into the utilization of various nano-composites, such as copper-, zinc-, and silver-based composites, among others, aiming to augment wood resistance against decay fungi and termites. Notable studies by Shiny et al. [10], Lykidis et al. [11], Terzi et al. [12], Mantanis et al. [13], Akhtari and Nicholas [14], and Clausen et al. [15], among others, have yielded promising results in this regard.

The application of silver nanoparticles (AgNPs) has become increasingly popular for enhancing diverse wood properties, including resistance to biological degradation, water absorption capacity, and dimensional stability. These improvements are achieved through both depth and surface treatments, spanning various concentrations of AgNPs [16–24].

For wood processing and protection purposes, the selection of AgNPs is underpinned by their distinct advantages over alternative options, including the aforementioned metal nanoparticles, chemical agents, and industrial-waste-derived antiseptics. These advantages encompass antimicrobial properties, durability enhancement, and a diminished environmental impact. In contrast to copper-based NPs or nanocomposites, AgNPs exhibit a more versatile antimicrobial application across diverse biological agents and disciplinary fields, showcasing efficacy on various materials and in different application formats [25]. Additionally, they demonstrate superior protective efficacy over time and at varying concentrations, although outcomes at lower concentrations may vary due to factors such as size, shape, application methods, and resistance to leaching [18,26–30]. Furthermore, the use of silver nanoparticles does not interfere with the deposition process or introduce defects in wood paint, offering a distinct advantage over copper nanoparticles that may potentially introduce harmful residues and defects [26]. Concerning zinc-based NPs or nanocomposites, although some studies underscore their effectiveness as a biocide, additional research is essential to fully comprehend their potential advantages and limitations,

as well as the underlying mechanisms governing their protective capabilities [31]. In the broader context of wood preservatives, AgNPs are deemed more environmentally friendly than traditional alternatives containing toxic chemicals that pose risks to human health and the environment [32]. Despite the notable drawback of AgNPs related to their higher synthesis and production cost, this limitation can be mitigated by exploring the minimum effective concentration and employing alternative synthesis strategies [33,34].

Chitosan, a natural and biodegradable polymer derived from the deacetylation of chitin, and its oligomers (COS) have also been investigated as protective solutions for wood due to their antimicrobial properties and harmlessness to human health and the environment. Their solutions, whether employed alone or in conjunction with nanoparticles (e.g., AgNPs), are primarily aimed at enhancing wood's durability against rotting fungi, yielding promising outcomes [18,19,35,36]. Chitosan's advantageous characteristics, including its low molecular weight, high water solubility, and elevated viscosity, contribute to its stabilizing properties. These attributes enable its efficient utilization in deep impregnation processes through vacuum-pressure application, with acceptable binding values [37]. Simultaneously, the chemical structure of chitosan, featuring amino ($-NH_2$) and hydroxyl ($-OH$) functional groups, equips it with chelating and reducing properties in the synthesis of AgNPs. This structural composition plays a crucial role in preventing the agglomeration of AgNPs [38].

In light of the aforementioned considerations, and with the current market increasingly emphasizing the use of wood products that align with the structural requirements outlined in Eurocode 5 (EN 1995-1-1:2016 [39]) concerning physical–mechanical performance and durability, nanotechnology emerges as a viable solution to enhance the inherent durability of wood, particularly in the case of *P. ×euramericana*. Therefore, building upon a preceding study [40], the primary objective of this research was to assess the efficacy of a binary composite consisting of AgNPs and COS in combating biodeterioration caused by white and brown rot fungi, as well as subterranean termites, in wood from *P. ×euramericana* 'I-214' treated through vacuum-pressure impregnation. Special emphasis has been placed on determining the minimum effective concentration of the preservative solution, aiming for economic efficiency.

The findings of this research contribute valuable insights to the field of wood preservation, aligning with the contemporary trend of seeking protective products that demonstrate greater consideration for environmental sustainability and human health [3,31,41].

2. Materials and Methods

2.1. Wood Material

Twenty-year-old *P. ×euramericana* 'I-214' wood originating from a commercial plantation situated in Quintanilla de Sollamas (42°36′00″ N, 05°49′00″ W), Castile-Leon, Spain, was utilized in this study. The material was received in the form of beams measuring 50 mm × 150 mm × 3000 mm, which were conditioned in the laboratory at approximately 65% relative humidity and 20 °C temperature, to achieve an equilibrium moisture content of 12 ± 2% (determined using a 606-1 digital hygrometer (Testo SE & Co. KGaA; Titisee-Neustadt, Germany)). The sampling and selection of test specimens (TSs) adhered to EN 350:2016 [1] standards for commercial sawn timber. In line with the findings by Spavento et al. [6], who found no significant differences between the inner and outer sections of wood, and considering that the selected beams of this commercial timber exhibited no evidence of heartwood, the TSs, in this case, were not differentiated based on the inner and outer sections of each beam. The beams were subsequently cut into defect-free specimens measuring 15 × 25 × 50 mm (thickness, width, and length, respectively), adhering to the standards EN 113-1-2:2021 [42,43] and EN 117:2012 [44] for decay fungi and termites, respectively.

In accordance with the validation requirements of the aforementioned standards, *Fagus sylvatica* L. (beech) and *Pinus sylvestris* L. (pine, sapwood) defect-free timber, adhering

to the same dimensions and sampling and selection criteria as outlined for the TSs, were employed as reference timber (RTs) for decay fungi and termites, respectively.

The treatments and number of repetitions per treatment are detailed in Table 1.

Table 1. Concentrations of each solution to obtain the binary composites and repetitions.

Treatments	Species	AgNPs (ppm)	COS (g·L^{-1})	Decay Fungi (Repetitions/ Fungal Species)	Termite (Repetitions)
Untreated	Poplar [a]	–	–	30	9
	Poplar [b]	–	–	30	9
	Beech [c]	–	–	30	–
	Pine [d]	–	–	–	9
AgNPs–COS$_{(4-20)}$		4	20	30	9
AgNPs–COS$_{(2-10)}$		2	10	30	9
AgNPs–COS$_{(1-5)}$	Poplar	1	5	30	9
AgNPs–COS$_{(0.5-2.5)}$		0.5	2.5	30	9
AgNPs–COS$_{(0.25-1.25)}$		0.25	1.25	30	9
	Total repetitions			480	72

[a] Control test specimen; [b] solvent (water) control specimen; [c,d] reference timber for rot fungi and termites, respectively.

2.2. Silver Nanoparticles and Chitosan Oligomers Composite Preparation

Chitosan oligomers were produced through enzymatic degradation following the procedure outlined by Buzón-Durán et al. [45], with adjustments as per the methods described by Ho et al. [46] and Santos-Moriano et al. [47]. In this process, 100 g of high-molecular-weight chitosan powder (CAS No. 9012-76-4; 310,000–375,000 Da), obtained from Caldic Ibérica S.L. (Barcelona, Spain), was dissolved in 5000 mL of Milli-Q water by incorporating 100 g of citric acid (CAS No. 77-92-9) with continuous stirring at 60 °C. Following complete dissolution, 1.67 g·L^{-1} of Neutrase® 0.8 L (supplied by Novozymes, Bagsvaerd, Denmark) was added to initiate the degradation of polymer chains. The solution underwent stirring at 40–60 °C for 12 h. Subsequently, it underwent a 5 min ultrasonication process in 1 min periods (employing a probe-type UIP1000hdT ultrasonicator; Hielscher, Teltow, Germany; 1000 W, 20 kHz), maintaining the temperature between 40 and 60 °C. At the conclusion of the procedure, a solution with a pH approximately equal to 4.5–5 and a molecular weight less than 2000 Da (determined through viscosity measurements) was obtained.

Silver nanoparticles were synthesized using an ultrasonication method. The process involved mixing 0.08 g of silver nitrate with 200 mL of *Chamaemelum nobile* (L.) All. solution (5% *v/v*) as a reducing agent. The mixture was stirred and heated at 40–60 °C under UV light until the solution transitioned from colorless to pale yellow, eventually intensifying (pH = 4.5–5). The yellowish solution underwent sonication for 3–5 min and was left to stand for at least 24 h in a refrigerator at 5 °C. The resulting AgNPs were characterized by transmission electron microscopy using a JEOL (Akishima, Tokyo, Japan) JEM-FS2200 HRP microscope.

Following EN 113-1:2021 [42] guidelines, a sufficient quantity of the highest concentration solution was prepared for both COS and AgNPs, aiming to generate, through dilution, a series of five concentrations spread around the anticipated toxic value (see Table 1). The concentrations for AgNPs, adhering to the reference method from EUCAST [48], were chosen based on previous in vitro findings as reported by Silva-Castro et al. [19,35].

For the binary solution, the COS and AgNP solutions were mixed, as specified in Table 1. Subsequently, ultrasonication for 5 min was applied to facilitate the formation of smaller and monodisperse COS particles [46,49].

2.3. Impregnation Method

The impregnation process followed the guidelines of EN 113-2:2021 [43], with certain modifications, such as adjustments to pressure conditions aimed at enhancing the absorption of treatment solutions (as indicated in the following paragraph). Prior to impregnation, each set of TSs for the AgNPs–COS treatment and the water control underwent oven drying until they reached an initial dry mass (m_0). Subsequently, they were stored in a desiccator to maintain dryness until the impregnation process.

The impregnation procedure involved placing the TSs in the treatment vessel, which was then positioned in the vacuum vessel equipped with a vacuum pump and stopcock. The pressure was reduced to 0.7 kPa and maintained for 15 min. Following this, the stopcock connected to the vacuum pump was closed, and another stopcock was opened to allow the preservative solution to be drawn into the treatment vessel within the vacuum environment. Air was then introduced, restoring the vacuum vessel to atmospheric pressure. Subsequently, another stopcock was opened to increase the pressure to 8 bar, deviating from the atmospheric pressure stipulated in EN 113-2:2021 [43]. This adjustment was made to replicate the Bethell industrial process and was sustained for a period of 2 h. Afterward, the TSs were extracted from the treatment vessel, excess liquid was removed by gently blotting with absorbent paper, and the TSs were immediately weighed to the nearest 0.01 g to determine the mass after impregnation (m_1).

Net absorption and retention were calculated using Equations (1) and (2), respectively.

$$NA = \frac{m_1 - m_0}{v}, \tag{1}$$

$$R = NA \times \frac{C}{100}, \tag{2}$$

where NA is the net absorption in $kg \cdot m^{-3}$; m_1 is the final mass (post-impregnation) in kg; m_0 is the initial dry mass (pre-impregnation) in kg; v is the volume in m^3; R is the retention of the active principle, AgNPs–COS, in $kg \cdot m^{-3}$; and C is the concentration in %.

2.4. Wood-Decay Fungi Resistance Tests

The assessment of poplar resistance to decay fungi was conducted following EN 113-1:2021 [42]. *Trametes versicolor* (L.) Lloyd (strain CTB 863 A) and *Coniophora puteana* (Schumach.) P.Karst. (strain BAM Ebw.15) served as the white and brown rot fungi, respectively. Each strain was cultivated in agar–malt medium (1.5% agar, 3% malt) in 350 mL glass dishes and incubated at $22 \pm 2\,°C$ with $70 \pm 5\%$ relative humidity (RH). Once covered by fungal tissue, the TSs and reference timber RT were introduced into the rot dishes, with two specimens per flask, after determining the initial dry mass (m_i) and autoclaving. Following 16 weeks under controlled temperature and humidity conditions ($22 \pm 2\,°C$ and $70 \pm 5\%$ RH), the samples were removed from the dishes, conditioned (superficial mycelium extraction), and oven-dried at $103 \pm 2\,°C$ to ascertain the final dry mass (m_f). Subsequently, the mass loss percentage (ML) was calculated using Equation (3).

$$ML = \frac{m_i - m_f}{m_i} \times 100 \tag{3}$$

where ML is the mass loss in %; m_i is the initial dry mass in g; and m_f is the final dry mass in g.

2.5. Termite Resistance Tests

The evaluation of poplar wood resistance to subterranean termites was conducted in accordance with standard EN 117:2012 [44], utilizing *Reticulitermes grassei* Clément as the biological material. The termite colonies consisted of 250 workers, accompanied by a small number of nymphs and soldiers, maintaining a ratio of 1 to 5%, mirroring the proportion found in the original colony from which the workers were sourced.

Each colony was situated in glass containers with a substrate of moist sand, comprising 1 part water and 8–10 parts sand. Additionally, 0.5 g of *Pinus* sp. wood shavings were evenly scattered on the substrate as the initial food source for the colonies. A glass ring was introduced against one of the vertical walls of the container, partially extending above the substrate surface. The containers were then incubated in a culturing chamber at 26 ± 2 °C with 70 ± 5% RH for a period of 2 to 4 days until the colony achieved uniformity and vitality. Following this, a wood specimen (TS or RT) was placed on the glass ring in each container, and the containers were further incubated in the chamber for 8 weeks, with periodic checks on the substrate humidity.

After the incubation period, the wood specimens were removed from each container, cleaned, and examined. The count of living termites (workers, nymphs, and soldiers) was recorded, and the attack ratings were visually assessed based on EN 117:2012 [44] criteria: (0) no attack; (1) attempted attack; (2) light attack; (3) medium attack; and (4) heavy attack. The survival rate (SR, %) was estimated using the ratio of the initial number of workers to the number of survivors. For the mean visual rating (VR), if more than 50% of samples fell into a specific class (e.g., heavy attack), the entire sample batch was assigned that class. The same methodology was applied to other attack criteria. Although not specified by the standard, the percentage of mass loss for the specimens was also evaluated using Equation (3).

2.6. Durability and Use Classes Assignment

The criteria for assessing resistance to deterioration induced by decay fungi and termites, along with their corresponding durability class (DC), are outlined in Table 2 (EN 350:2016 [1]). The use class was estimated in accordance with standard EN 335:2013 [50].

Table 2. Durability class (DC) against the attack of decay fungi and termites.

Decay Fungi			Termites		
DC	Description	Median ML (%) EN 350:2016	DC	Description	Attack Level * EN 350:2016
1	Very durable	≤ 5	D	Durable	>90% '0 o 1' and maximum 10% '2' *
2	Durable	>5 to ≤ 10	M	Moderately durable	<50% '3, 4'
3	Moderately durable	>10 to ≤ 15			
4	Slightly durable	>15 to ≤ 30	S	Not durable	>50% '3, 4'
5	Not durable	>30			

* 90% of test specimens classified as '0' or '1', with a maximum of 10% of test specimens classified as '2', and no test specimens classified as '3' and '4'.

2.7. Microstructural Alterations and Microanalysis with SEM–EDS

To investigate fungal degradation and termite attack, and to study the multi-elemental composition of the wood, small sections (approximately 2×3 mm) from specimens subjected to *T. versicolor* and *C. puteana* for 16 weeks and to *R. grassei* for 8 weeks were analyzed using scanning electron microscopy (SEM) and an energy-dispersive X-ray spectrometer (EDS). The specimens included those treated with AgNPs at 4 ppm + COS at 20 g·L^{-1} (provided that it was the concentration that led to the best results in protection tests) and untreated control test specimens.

Specimen sections, obtained from both the transverse and longitudinal planes, were prepared with disposable blades, and mounted on slides using bifacial tape. Observations were conducted using an ESEM Quanta 250 FEG (FEI Company, Thermo Fisher Scientific; Waltham, MA, USA) microscope equipped with an electron probe microanalysis unit and an Oxford Instruments (Abingdon, UK) 5DD X-Act model EDS. The analyses were performed

at the Scanning Electron Microscopy and Microanalysis Service of the LIMF (Facultad de Ingeniería, Universidad Nacional de La Plata, Buenos Aires, Argentina).

2.8. Statistical Analysis

Statistical analyses were performed using R software (version 4.2.2) [51]. Of the total number of trials carried out by wood species and treatments (Table 1), 236, 234, and 72 data values were subjected to analysis for white, brown, and termite rot, respectively. The statistical assumptions of independence, normality, and homoscedasticity were thoroughly assessed. Normality and homoscedasticity were evaluated using the Shapiro–Wilks test and either the Bartlett or Levene test, respectively. Based on these assessments, a comparative analysis of linear statistics (ANOVA) and robust statistics (Welch) with (or without, as appropriate) the bootstrapping trimmed means method was applied to determine the equality of medians and means, respectively, and to identify homogeneous groups.

3. Results

3.1. Impregnation and Efficacy of Treatments against Biological Agents

The solutions of the binary composite formulated at various concentrations of AgNPs and COS are illustrated in Figure 1a. The characterization of the AgNPs revealed a predominantly spherical morphology with an average diameter of 20 ± 6 nm (Figure 1b).
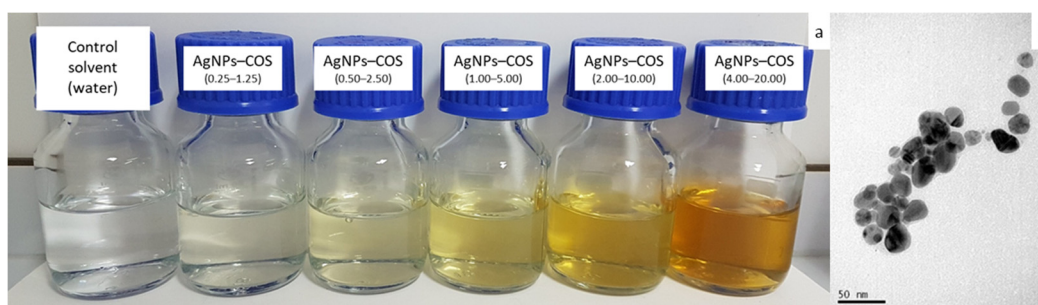

Figure 1. (**a**) AgNPs–COS solutions; (**b**) TEM micrograph of the synthesized AgNPs.

Table 3 presents the results of the impregnation process along with the density values of samples for each treatment. Figure 2 illustrates, for each biological agent, the retention behavior of the active principle (AgNPs–COS) concerning the concentrations applied, revealing a significant and exponentially increasing relationship between the two.
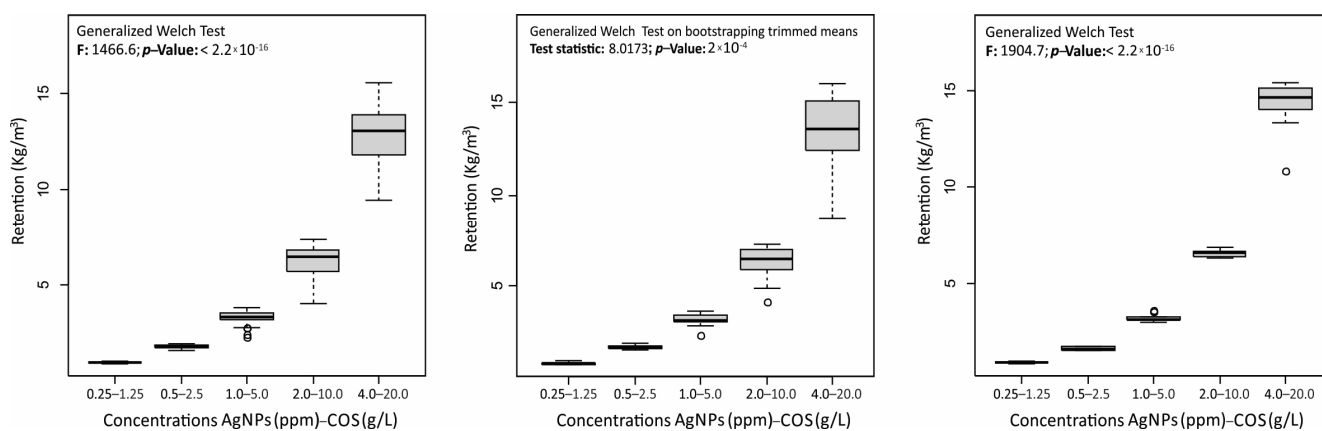

Figure 2. Retention vs. treatment in poplar wood by biological agent. From left to right: white rot, brown rot, and termite.

Table 3. Descriptive analysis of density and impregnation process results by biological agent.

Treatment *	Species	Density † (kg·m⁻³) ± IC *			Net Absorption (kg·m⁻³) ± IC *			Retention (kg·m⁻³) ± IC *		
		Wr **	Br **	T **	Wr **	Br **	T **	Wr **	Br **	T **
Untreated	Poplar [a]	418.50 ± 18.24	436.57 ± 18.29	411.11 ± 17.72	–	–	–	–	–	–
	Poplar [b]	419.01 ± 15.50	426.64 ± 16.15	383.16 ± 22.32	717.17 ± 15.66	733.40 ± 10.89	750.11 ± 13.77		–	–
	Beech [c]	659.08 ± 6.41	669.67 ± 13.41	–	–	–	–	–	–	–
	Pine [d]	–	–	467.10 ± 13.34	–	–	–	–	–	–
AgNPs–COS$_{(4–20)}$	Poplar	376.75 ± 12.08	372.93 ± 12.78	403.17 ± 16.92	643.59 ± 27.06	680.64 ± 32.82	713.22 ± 46.82	12.87 ± 0.54	13.62 ± 0.66	14.27 ± 14.27
AgNPs–COS$_{(2–10)}$		391.59 ± 13.33	401.43 ± 16.04	409.27 ± 37.16	613.41 ± 32.46	632.37 ± 29.11	654.60 ± 13.22	6.14 ± 0.33	6.33 ± 0.29	6.55 ± 0.13
AgNPs–COS$_{(1–5)}$		404.02 ± 13.01	405.91 ± 13.74	417.04 ± 31.86	651.02 ± 26.44	647.63 ± 20.08	646.00 ± 29.17	3.26 ± 0.13	3.24 ± 0.10	3.23 ± 0.15
AgNPs–COS$_{(0.5–2.5)}$		374.11 ± 11.73	385.01 ± 12.72	367.69 ± 16.39	691.55 ± 12.82	694.69 ± 15.04	649.14 ± 29.17	1.73 ± 0.03	1.74 ± 0.04	1.62 ± 0.06
AgNPs–COS$_{(0.25–1.25)}$		374.39 ± 8.93	377.42 ± 10.13	388.66 ± 24.84	728.79 ± 9.85	691.87 ± 15.20	726.17 ± 20.34	0.91 ± 0.03	0.87 ± 0.02	0.91 ± 0.03

[a] Control test specimen; [b] solvent (water) control specimen; [c,d] reference timber for decay fungi and termites (beech and pine, respectively); * IC = robust confidence intervals; ** Wr = white rot, Br = brown rot, T = termite.
† Density measured with 12% moisture content.

The assessment of treatment efficacy (untreated vs. treated wood) against *T. versicolor* (Wr), *C. puteana* (Br), and *R. grassei* (T) is summarized in Table 4, Table 5, and Table 6, respectively. The validity of the tests was confirmed in the reference treatments (RTs). For *T. versicolor* and *C. puteana*, this validation was corroborated in beech samples through weight loss exceeding 15% and 20%, respectively (according to EN 113-1:2021 [42]). In the case of *R. grassei*, the validation was conducted in pine samples using a visual attack criterion (VR) of '4' and a survivor rate (SR) exceeding 50% (as per EN 117:2012 [44]).

Table 4. Comparative analysis of mass loss due to white rot for each treatment.

Treatments	Species	ML * (%) ± CI	S–W Test * p-Value	B Test * p-Value	ANOVA p-Value	Homogenous Groups **
Untreated	Poplar [a]	41.96 ± 4.49	0.194			a
	Poplar [b]	40.46 ± 3.06	0.502			a
	Beech [c]	42.01 ± 4.97	0.274			a
AgNPs–COS$_{(4–20)}$	Poplar	30.15 ± 3.08	0.650	0.089	7.44×10^{-5}	b
AgNPs–COS$_{(2–10)}$		36.76 ± 3.87	0.047			ab
AgNPs–COS$_{(1–5)}$		41.49 ± 4.80	0.207			a
AgNPs–COS$_{(0.5–2.5)}$		40.69 ± 4.66	0.753			a
AgNPs–COS$_{(0.25–1.25)}$		45.44 ± 4.48	0.682			a

[a] Control test specimen; [b] solvent (water) control specimen; [c] reference timber (beech); * ML = mass loss, CI = confidence interval, S–W = Shapiro–Wilk test, B = Bartlett test; ** Significant differences between treatments are indicated by different letters (Tukey test $p < 0.05$).

Table 5. Comparative analysis of mass loss due to brown rot for each treatment.

Treatments	Species	ML * (%) ± CI	S–W Test * p-Value	Lv Test * p-Value	W Test * p-Value	Homogenous Groups **
Untreated	Poplar [a]	41.93 ± 4.33	0.085			cd
	Poplar [b]	47.86 ± 3.26	0.048			b
	Beech [c]	40.57 ± 3.46	0.001			d
AgNPs–COS$_{(4–20)}$		27.22 ± 0.66	0.000			a
AgNPs–COS$_{(2–10)}$		49.90 ± 3.26	0.000	1.604×10^{-7}	2×10^{-4}	b
AgNPs–COS$_{(1–5)}$	Poplar	47.69 ± 4.25	0.048			bc
AgNPs–COS$_{(0.5–2.5)}$		50.34 ± 3.44	0.000			b
AgNPs–COS$_{(0.25–1.25)}$		48.99 ± 3.78	0.043			b

[a] Control test specimen; [b] solvent (water) control specimen; [c] reference timber (beech); * ML = mass loss, CI = robust confidence interval, S–W = Shapiro–Wilk Test, Lv = Levene Test, W = Welch Test; ** Significant differences between treatments are indicated by different letters (post hoc test on bootstrapping trimmed means, $p < 0.05$).

Table 6. Comparative analysis of visual rating, survival rate, and mass loss caused by termites for each treatment.

Treatments	Species	VR *	SR * (%)	ML * (%) ± CI	S–W Test * p-Value	B Test * p-Value	ANOVA p-Value	Homogenous Groups ** SR	Homogenous Groups ** ML
Untreated	Poplar [a]	4	53.98 ± 10.40	15.04 ± 1.20	0.898			a	b
	Poplar [b]	4	55.57 ± 3.67	22.29 ± 3.40	0.868			a	a
	Pine [c]	4	56.34 ± 9.03	13.85 ± 2.48	0.150			a	b
AgNPs–COS$_{(4–20)}$		1	26.62 ± 8.63	7.95 ± 1.03	0.897	0.0495	5.65×10^{-12}	b	d
AgNPs–COS$_{(2–10)}$		4	34.03 ± 7.65	8.55 ± 2.08	0.836			b	d
AgNPs–COS$_{(1–5)}$	Poplar	4	36.43 ± 8.29	9.82 ± 2.36	0.147			b	cd
AgNPs–COS$_{(0.5–2.5)}$		4	42.85 ± 6.67	14.94 ± 2.56	0.093			ab	bc
AgNPs–COS$_{(0.25–1.25)}$		4	50.19 ± 4.74	11.94 ± 2.19	0.365			ab	b

[a] Control test specimen; [b] solvent (water) control specimen; [c] reference timber (pine); * VR = visual rating, SR = survival rate, ML = mass loss, CI = confidence interval, S–W: Shapiro–Wilk test, B = Bartlett test; ** Significant differences between treatments are indicated by different letters ($p < 0.05$).

Consistently, across all cases, the formulation featuring 4 ppm AgNPs and 20 g·L^{-1} of COS was the only treatment that significantly enhanced resistance to decay caused by Wr, Br, and T. This particular formulation led to noteworthy reductions in weight loss compared to untreated poplar wood (control test specimen), with percentage values of 28, 35, and 47%, respectively. In the case of T, the degree of attack was also diminished, reaching level '1', corresponding to a survival rate of approximately 27%, showcasing a declining trend with increasing concentration (refer to Figure 3).

Based on the obtained results and considering the criteria for assigning durability class (DC) outlined in EN 350:2016 [1] (Table 2), poplar wood impregnated with the solution containing 4 ppm AgNPs and 20 g·L^{-1} of COS demonstrated enhanced resistance against *C. puteana*, progressing from DC '5' (not durable, as per Spavento et al. [6]) to DC '4' (not very durable). Although there was no observed improvement in DC against *T. versicolor* attack, it nearly reached the threshold between DC '5' and DC '4' (30%). Furthermore, resistance to termite attack was enhanced, moving from DC 'S' (not durable) to DC 'M' (moderately durable).
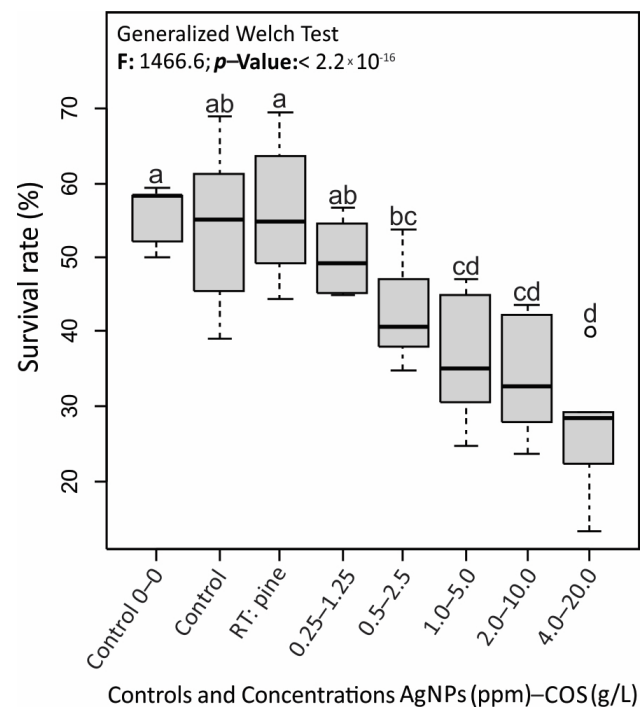
Figure 3. Survival rate behavior. Significant differences between treatments are indicated by different letters ($p < 0.05$).

3.2. Microstructural Alterations and Material Microanalysis

Wood samples subjected to both xylophagous fungal strains, with and without treatment (AgNPs 4 ppm + COS 20 g·L^{-1} and control test specimen, respectively), exhibited microstructural alterations, confirming the diagnosed degradation based on mass loss.

In sections of specimens attacked by *T. versicolor*, predominant alterations included the thinning and deformation of the vessel wall, holes in radial parenchyma, the collapse of the ray sectors, the presence of erosion trails/channels in all cell types, and the erosion of the ray-vessel pits and fibers. Notably, a high concentration of mycelium was observed in the vessels and sectors of tissue that had completely collapsed, displaying a fibrillar aspect (see Figure 4). The material exhibited a corky consistency, more pronounced in the control specimens.

In specimens exposed to *C. puteana*, identified alterations comprised tissue deformation, fractures in all cell types, and the presence of mycelium mainly in the vessels of untreated wood (refer to Figure 5). These samples were characterized by their brown coloration and brittleness.

In all instances, the impregnated material exhibited lower severity and extent of microstructural alterations in the tissue, a finding consistent with the recorded percentages of mass loss.

Furthermore, white deposits were identified in wood sections from both treatments (AgNPs 4 ppm + COS 20 g·L^{-1} and control test specimen) and both biological agents (Wr and Br). These deposits, observed as isolated particles or forming aggregates, were present in various cell types and associated with evidence of colonization and fungal degradation. They were notably abundant in the vessels of the control wood attacked by *C. puteana* (see Figure 5B,C).

Concerning the material subjected to termite attack, SEM-identified alterations, such as mechanical damage and the tearing of the woody tissue, aligned with descriptions by Spavento et al. [6]. These alterations were less severe in the impregnated wood, consistent with its lower shrinkage and greater resistance observed when pressed between the fingers.
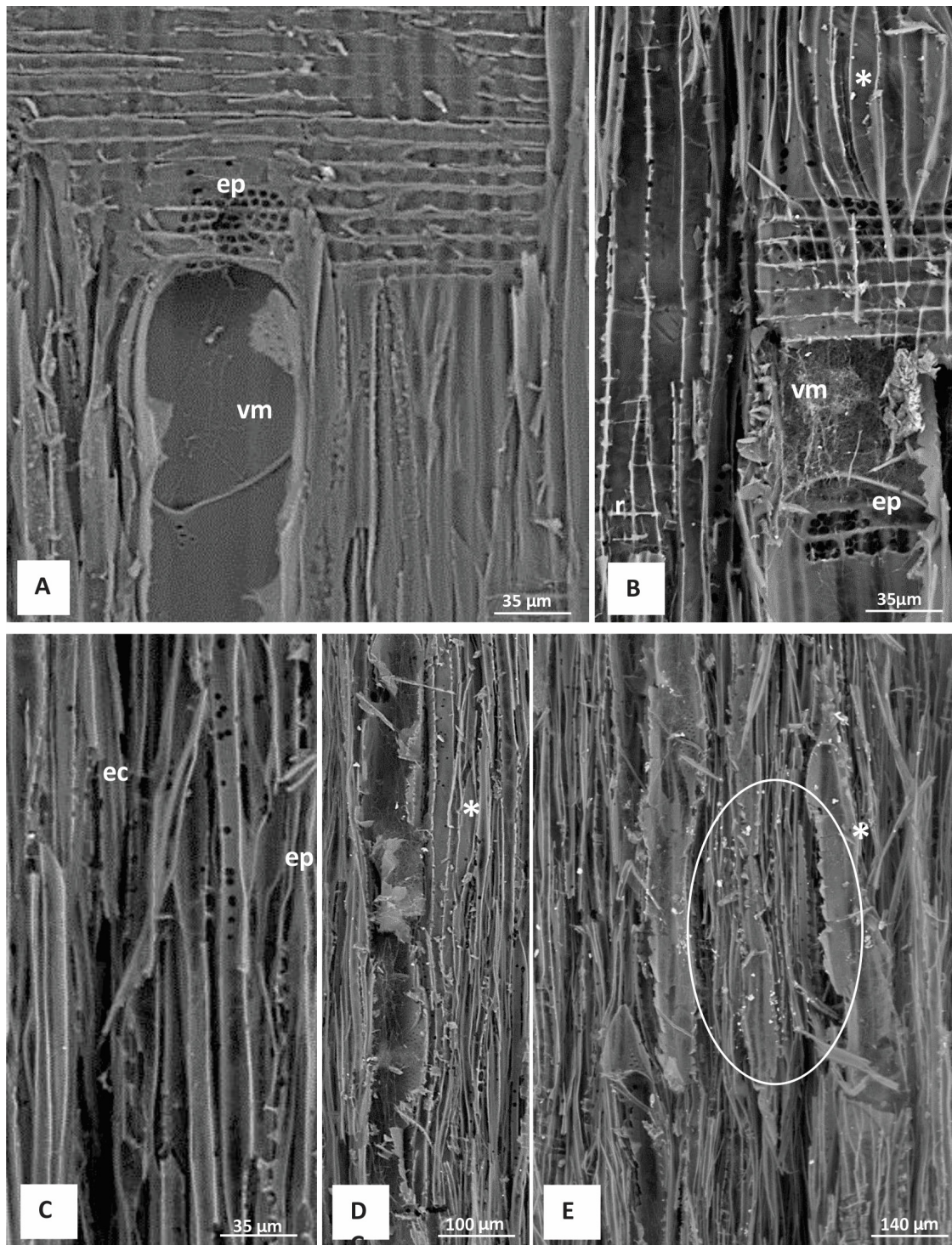
Figure 4. Microstructural alterations in wood exposed to *Trametes versicolor* (L.) Lloyd. (**A**) Impregnated wood. Scarce mycelium in the vessel and incipient erosion in the vessel-radius pits (radial longitudinal view). (**B–E**) Untreated wood. (**B**) Abundant mycelium in vessel element, erosion in ray-vessel pits, collapse of radial parenchyma cells, and deposits in fiber wall (radial longitudinal view). (**B**) Erosion path/channel and eroded pits in fibers (tangential longitudinal view). (**D,E**) Fibrillar appearance of tissue and presence of deposits (radial longitudinal view and tangential longitudinal view, respectively). vm = Vessel mycelium, ep = eroded pit; r = parenchymal radius; ec = erosion path/channel, * = deposits.
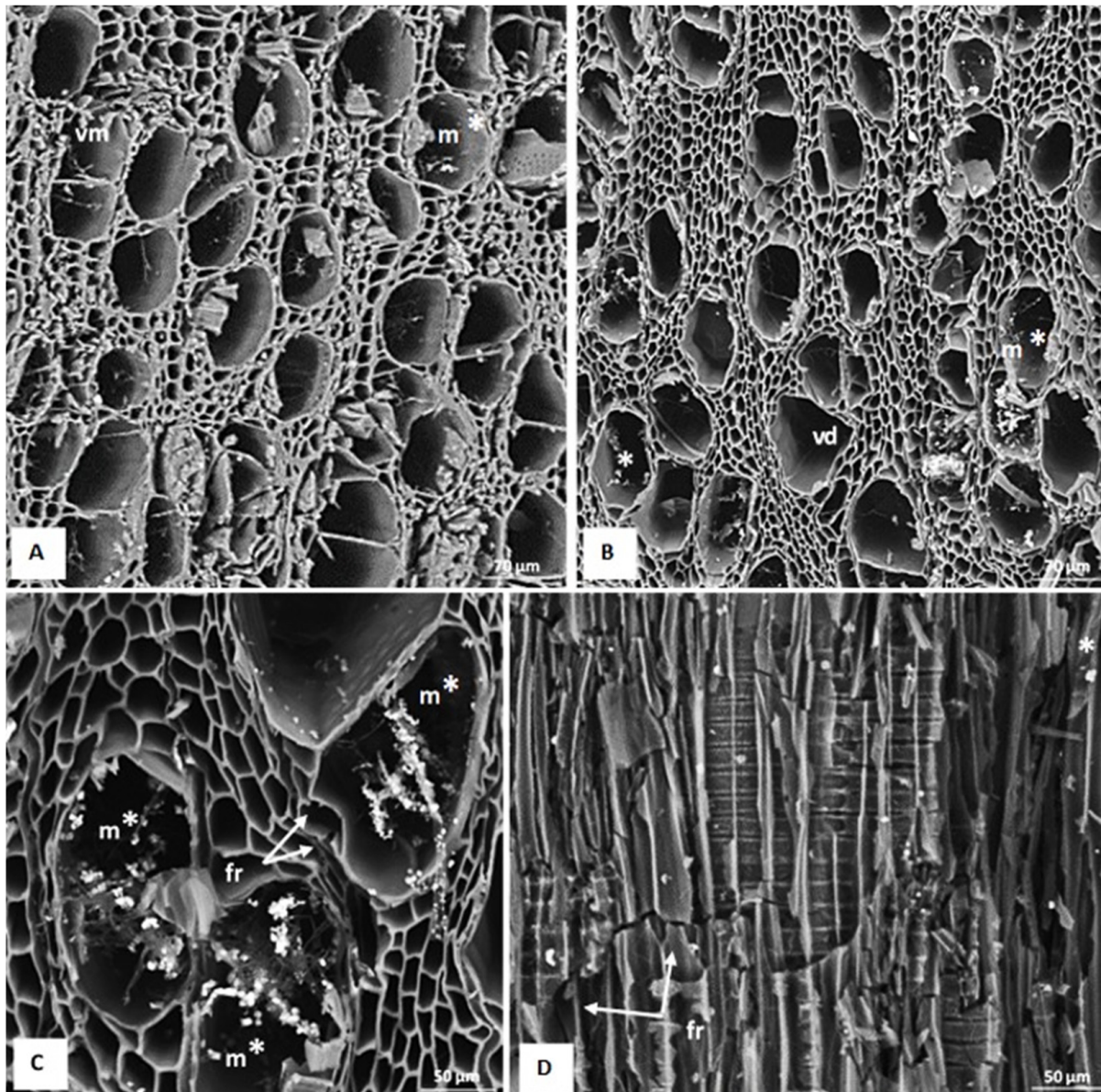
Figure 5. Microstructural alterations in wood exposed to *Coniophora puteana* (Schumach.) P.Karst. (**A**) Impregnated wood. Vessels with mycelium and sparse deposits (transverse view). (**B**–**D**) Untreated wood. (**B**,**C**) Mycelium and deposits in vessels, general aspect, and detail, respectively, and fractures in fiber (transverse view). Note the deformation of the vessels with respect to the treated material and the higher concentration of mycelium and deposits. (**D**) Fracture perpendicular and transverse to the grain, and deposits (longitudinal radial view). v = Vessel element, m = mycelium, d = deformation, fr = fracture, * = deposits.

With EDS, AgNPs were not identified in the bulk material treated with the binary composite. In the control and impregnated samples exposed to both types of rot, the elements present in different sectors of the tissue (vessels, fibers, and rays with and without evidence of attack) were C and O with the highest concentrations, followed by Cu, Ca, K, Zn and, to a lesser extent, Cl, P, Na, Si, S, and Mg. In all the treatments, a trend towards an increase in Ca concentration was identified in the areas with evidence of colonization and fungal degradation and the presence of deposits. Particularly accentuated was the increase in Ca in the vessel lumens of the control specimens exposed to brown rot (Figure 6).
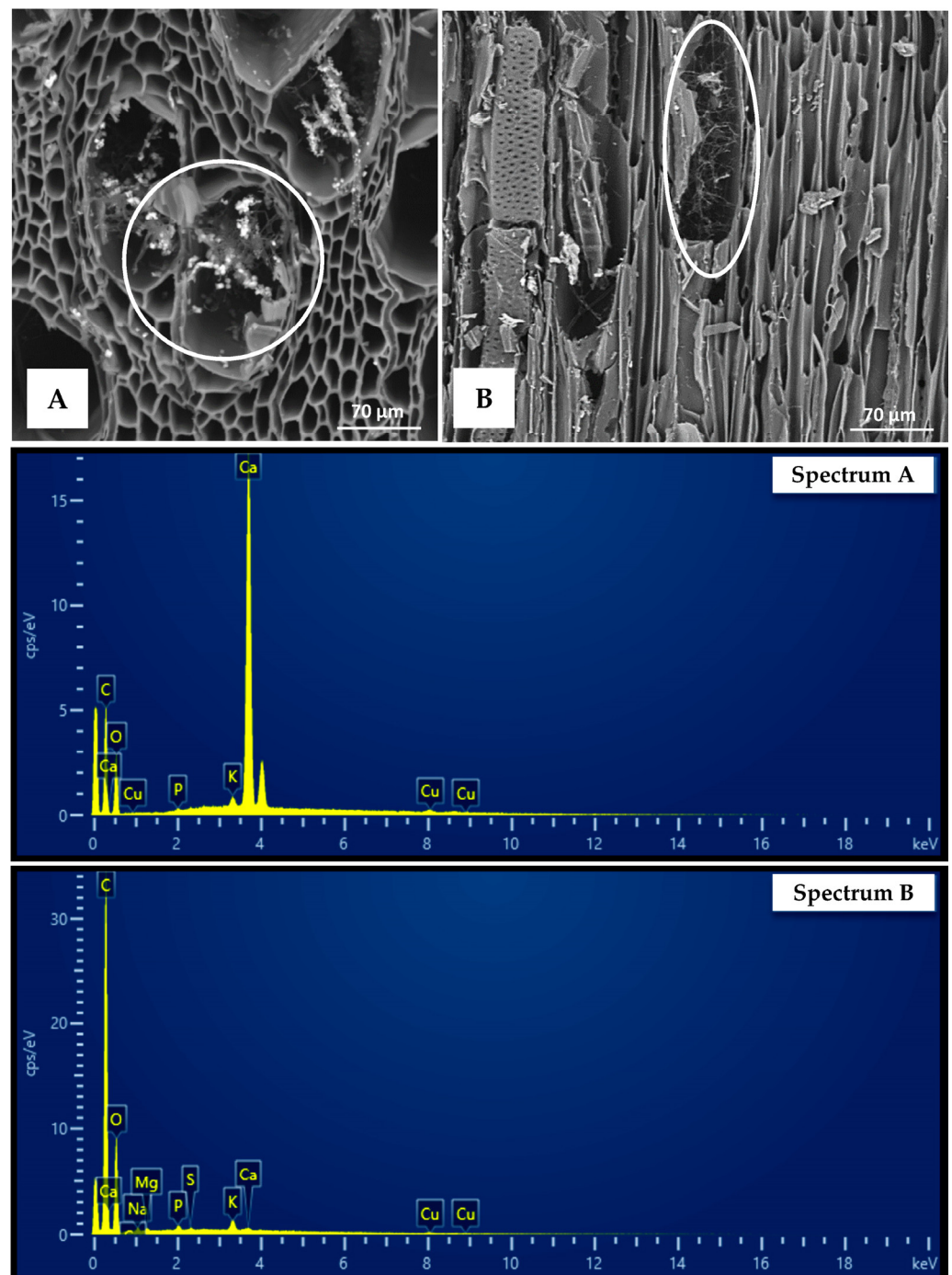
Figure 6. Sections of specimens exposed to brown rot analyzed with SEM–EDS along with the EDS spectra of the circled regions. (**A**) Deformed vessels with mycelium and deposits (transverse view). (**B**) Sector of vessel element with abundant mycelium lacking deposits (tangential longitudinal view). Note the difference in Ca percentage.

4. Discussion

4.1. Efficacy of Treatments against Biological Agents

The effectiveness of the binary solution containing AgNPs–COS on *P.* ×*euramericana* 'I-214' wood from Spain was discernible only at the highest concentration (4 ppm + 20 g·L^{-1}), particularly against *C. puteana* and *R. grassei*.

In terms of efficacy against *T. versicolor*, the results obtained in this study were less favorable than those reported by Casado et al. [18] in poplar wood treated through vacuum-

pressure impregnation of AgNPs solutions at 5 ppm after 16 weeks (ML = 8.94% vs. 30.15% in this study). Moya et al. [20,21] also observed enhanced resistance to degradation by *T. versicolor* in 12 tropical commercial wood species treated with a solution of AgNPs. Weight loss percentages ranged from 7 to 11% after four months, which were lower than those reported herein, but it is worth noting that a significantly higher concentration (50 ppm AgNPs + ethylene glycol) was employed. However, their results were notably less promising against the brown rot causal agent *Lenzites acutus* Berk. (=*Cellulariella acuta* (Berk.) Zmitr. & Malysheva), with weight loss values in the 8 to 35% range (vs. 27.22% for *C. puteana* at 4 ppm in this study). These researchers also noted improved dimensional stability and reduced water absorption capacity in the treated wood. Pařil et al. [30] reported similar outcomes in beech and pine wood treated with AgNP solutions, with weight losses below 3%, although at much higher AgNP concentrations (1000 ppm and 3000 ppm), when tested against *T. versicolor* and *Poria placenta* (Fr.) Cooke (=*Rhodonia placenta* (Fr.) Niemelä, K.H.Larss. & Schigel; brown rot), respectively. Considering the literature, the relatively low efficacy against *T. versicolor* observed in this study could be attributed to the chosen AgNP concentrations, which were substantially lower than those employed by the cited authors, particularly through deep impregnation.

Regarding the mechanism of action, the reduction in weight loss in both white rot and brown rot cases might be attributed to different factors. AgNPs exposed to high humidity exhibit remarkable antifungal activity. In this process, metallic silver undergoes oxidation in the presence of water, leading to the release of ions. These silver ions, when in solution, significantly impact the exoenzymatic activity of both white and brown rot fungi. As elucidated by Dorau et al. [24], their specific influence is notable in the activity of cellulase enzymes produced by decay fungi. Given the inherently slow nature of this chemical reaction transformation, the particle size assumes critical importance in inhibiting fungal growth. Consequently, smaller particle sizes result in a higher specific surface area and enhanced oxidation effectiveness, providing more effective protection against these spoilage agents through the sustained slow release of silver ions [27]. Additionally, AgNPs, particularly those of smaller sizes, can induce the generation of reactive oxygen species (ROS) and free radicals within cells, leading to oxidative stress and, ultimately, cell death. These AgNPs enter cells through proton pumps, disrupting their function and that of the electron transport chain, resulting in an increased production of ROS and subsequent damage to proteins, lipids, and nucleic acids [34,52,53]. Furthermore, AgNPs have been identified to hinder the DNA replication process. Another mechanism involves the interaction between AgNPs and thiol groups of proteins, leading to the deactivation of the latter [54]. AgNPs may also adhere to cell surfaces, compromising membrane integrity and function [55]. Importantly, these mechanisms are considered to operate simultaneously, representing multiple modes of action rather than functioning in isolation [54].

Concerning termites, the existing literature on nanotechnology as a strategy to enhance resistance against this form of deterioration primarily focuses on coniferous wood. Additionally, studies explore the application of chemical elements such as zinc oxides, borates, and copper oxides, either independently or in combination with AgNPs, usually at concentrations not surpassing 2% [13,14,23]. However, the outcomes from these investigations align closely with the findings obtained in the current study.

Regarding the mortality rate, the one observed with the AgNPs-COS (4 ppm–20 g·L^{-1}) solution (73.38%, SR = 26.62%) closely resembled those documented by Green and Arango [23] for 0.5% nano zinc oxide + Ag (76%). However, it was lower than the rate reported by Mantanis et al. [13] for formulations containing 2% nano zinc oxide (>90%).

As per Green and Arango [23], instances where a high survival rate was observed could be attributed to repellency or avoidance rather than direct toxicity. It is worth considering that, in general, the effectiveness of AgNPs against biological degradation agents might hinge on nanoparticle characteristics, such as size and shape, influencing their performance in wood protection applications concerning adhesion and internalization [15,56]. Can et al. [57] propose that achieving effective protection through the slow release of silver

ions requires particles to be less than 100 nm in size. Additionally, Bugnicourt et al. [58] suggest that spherical-shaped nanoparticles, as obtained in this study (Figure 1b), enhance the internalization into cells. Conversely, Jafernik et al. [56] point out that non-spherical NPs might have a greater impact on transmission, circulation, transfer, and distribution.

The stability of the solution is another crucial aspect, alongside the shape and size of the nanoparticles. As previously mentioned, the characteristics of chitosan (COS), including high water-solubility and viscosity, coupled with its chemical structure featuring chelating and reducing groups, play a crucial role in preventing agglomeration. This combination ensures a more effective stabilization of the solution [35,38,59–62].

Chitosan oligomer nanoparticles (COS NPs) have been explored as wood protective solutions, either alone or in combination with other nanoparticles (e.g., AgNPs), to enhance the durability of wood against mold fungi, brown-rot, and white-rot fungi, consistently yielding promising results in various studies [18,19,35,36,63–65].

The inference that the decrease in weight loss and the subsequent improvement in resistance to degradation, especially against the brown-rot strain and termites in *P. ×euramericana* 'I-214' wood from Spain, is linked to the combined biocidal action of AgNPs–COS and appears valid based on the information provided. The prolonged efficacy observed after 16 or 8 weeks of trials, respectively, is attributed to the size and shape of the AgNPs and the stabilizing property of COS. This combination leads to a slow and/or controlled release of AgNPs, the primary bioactive compound of the binary solution, within the wood. This suggests a comparative advantage of the AgNPs–COS solution, aligning with the observations of Casado et al. [18].

Moreover, the promising results in improving durability class against deterioration caused by *C. puteana* are noteworthy. This improvement is significant, given the detrimental impact of brown rot on wood's resistance capacity, a critical property influencing its useful life in structural applications.

4.2. Microstructural Alterations and Material Microanalysis

The microstructural alterations observed in the wood subjected to different treatments (control and AgNPs–COS (4 ppm + 20 g·L^{-1})) and fungi (white rot and brown rot) align with the degradation identified by mass loss and the type of rot to which they were exposed. The modifications observed in test specimens degraded by *T. versicolor* and *C. puteana* are consistent with the diagnostic characteristics of white and brown rot, respectively.

White rots typically involve the degradation of the main polymers of the cell wall (holocellulose and lignin), resulting in structural alterations, a fibrillar aspect, and corky to spongy consistency in advanced stages of rot. These traits were detected in the material exposed to *T. versicolor*. On the other hand, brown rots involve holocellulose degradation and partial oxidation of lignin, leading to a brittle consistency, cubic fracture pattern, and brown color. These characteristics were identified in the test specimens exposed to *C. puteana*.

Concerning the EDS results, the absence of detectable AgNPs in the treated wood could be attributed to their low concentration in the binary solution (4 ppm). Elemental microanalysis findings, particularly the identification of peaks or increases in calcium concentration in sectors with evidence of colonization and degradation and the presence of deposits, may result from the precipitation of this element due to the biochelation phenomena caused by fungal acids. Xylophagous fungi, particularly those responsible for brown rot, produce high amounts of oxalic acid and chelating polycarboxylic acids, leading to the immobilization of metals in the form of insoluble oxalate crystals. The production of calcium oxalate is associated with wood degradation [66,67]. Rudakiya and Gupte [67] corroborate the presence of oxalate crystals, particularly with a high percentage of calcium.

The notable reduction in calcium percentage observed in wood sectors displaying evidence of decay and the absence of deposits may be attributed to a decrease in oxalic acid concentration. Several authors have noted that the disappearance of calcium oxalate crystals correlates with a decline in oxalic acid levels. Mechanisms such as nutrient depletion,

metabolic changes, the assimilation of oxalic acid as a carbon source, and the enzymatic degradation of oxalic acid are proposed explanations for the absence of calcium oxalate crystals and the subsequent decline in calcium percentage [66,68,69].

4.3. Applications and Limitations of the Study, and Further Research

In concordance with established research in wood preservation, the outcomes of this study underscore the potential of emerging technologies as eco-friendly alternatives to mitigate wood deterioration, extend its service life, and broaden the utility of less naturally durable wood, such as *P.* ×*euramericana* clone I-214.

While the results show promise, improving the durability class against the aggressive termites and brown rot strain, and notably reducing mass loss with the white-rot strain, a limitation surfaced in the inability to widen the classification gap compared to untreated wood. This highlights the necessity for the further refinement of treatment concentrations.

Aligned with the structural requirements set by Eurocode 5 (EN 1995-1-1:2016 [39]), ongoing research is dedicated to a comprehensive evaluation of the treated wood's resistance, considering the solutions and concentrations presented in this work. This evaluation encompasses the wood's resilience against deterioration caused by micro-fungi soft rot, as well as its elastic-resistant behavior pre- and post-treatment and fungal exposure. Moreover, to confirm treatment effectiveness and assess its broad applicability and reproducibility, there is a consideration to extend the study to other wood species with low natural durability and wide distribution (*Salix* spp., *Pinus pinaster* Aiton, and *Quercus* spp., among others), along with exploring fungal strains of significance in the wood industry (*Gloephylum* spp. and *Picnoporus* spp., among others).

5. Conclusions

The binary solution of AgNPs–COS, at concentrations of 4 ppm and 20 g·L^{-1}, respectively, significantly enhanced the resistance to decay induced by *T. versicolor*, *C. puteana*, and *R. grassei* in *P.* ×*euramericana* 'I-214' wood of Spanish origin when impregnated by vacuum pressure. Particularly noteworthy was the increase in the durability class achieved against *C. puteana* and *R. grassei*. Scanning electron microscopy studies provided visual confirmation of the treatment's effectiveness, revealing discernible differences between the control and treated wood in the severity and extent of tissue degradation. This work contributes significant evidence supporting the effectiveness against the biological deterioration of the AgNPs–COS composite at low concentrations when introduced via vacuum pressure. This treatment aligns with the characteristics of an 'ideal preservative', showcasing the capacity to respond effectively to preservation methods, exerting an impact on various organisms at low concentrations of the active principle, featuring slow release and prolonged action, and demonstrating environmental friendliness, among other desirable attributes. Furthermore, valuable insights are provided regarding its impact on degradation caused by a strain of *C. puteana*, an aspect that has been less explored to date but holds importance considering the influence of such deterioration on the wood's structural resilience.

Author Contributions: Conceptualization, E.S., M.T.d.T.-F., L.A.-R. and P.M.-R.; methodology, E.S., M.T.d.T.-F., M.M., S.M.S., M.C.-S., J.M.-G. and J.Á.-M.; formal analysis, E.S. and L.A.-R.; investigation, E.S., M.T.d.T.-F., S.M.S., R.D.M.-L., J.M.-G., J.Á.-M. and P.M.-R.; resources, E.S., M.T.d.T.-F., M.C.-S., R.D.M.-L., J.M.-G. and J.Á.-M.; writing—original draft preparation, E.S., M.T.d.T.-F., L.A.-R., M.M. and P.M.-R.; writing—review and editing, E.S. and P.M.-R.; visualization, M.C.-S., R.D.M.-L. and J.Á.-M.; supervision, M.T.d.T.-F., L.A.-R. and P.M.-R.; funding acquisition, E.S., M.T.d.T.-F. and M.C.-S. All authors have read and agreed to the published version of the manuscript.

Data Availability Statement: Data are contained within the article.

References

1. *EN 350:2016*; Durability of Wood and Wood-Based Products—Testing and Classification of the Durability to Biological Agents of Wood and Wood-Based Materials. European Committee for Standardization: Brussels, Belgium, 2016; p. 67.
2. Martín, J.A.; López, R. Biological deterioration and natural durability of wood in Europe. *Forests* **2023**, *14*, 283. [CrossRef]
3. Zabel, R.A.; Morrell, J.J. Wood deterioration agents. In *Wood Microbiology*, 2nd ed.; Zabel, R.A., Morrell, J.J., Eds.; Academic Press: San Diego, CA, USA, 2020; pp. 19–54. [CrossRef]
4. Tucker, C.L.; Koehler, P.G.; Pereira, R.M. Development of a method to evaluate the effects of eastern subterranean termite damage to the thermal properties of building construction materials (Isoptera: Rhinotermitidae). *Sociobiology* **2008**, *51*, 589–600.
5. Garnica, J. La importancia del chopo en la industria. In Proceedings of the Jornadas de Salicáceas-V Congreso Internacional de Salicáceas, Talca, Chile, 13–17 November 2017; p. 22.
6. Spavento, E.; Murace, M.; Acuña Rello, L.; Monteoliva, S.-E.; Troya Franco, M.T.D. Susceptibility of *Populus × euramericana* 'I-214'of Spanish origin to xylophagous attacks: Durability tests for its possible inclusion in European standard. *For. Syst.* **2019**, *28*, e008. [CrossRef]
7. Papadopoulos, A.N. Nanotechnology and wood science. *Nanomaterials* **2023**, *13*, 691. [CrossRef] [PubMed]
8. Bi, W.; Li, H.; Hui, D.; Gaff, M.; Lorenzo, R.; Corbi, I.; Corbi, O.; Ashraf, M. Effects of chemical modification and nanotechnology on wood properties. *Nanotechnol. Rev.* **2021**, *10*, 978–1008. [CrossRef]
9. Papadopoulos, A.N.; Kyzas, G.Z. Nanotechnology and wood science. In *Interface Science and Technology*; Kyzas, G.Z., Mitropoulos, A.C., Eds.; Elsevier: Amsterdam, The Netherlands, 2019; Volume 30, pp. 199–216.
10. Shiny, K.S.; Sundararaj, R.; Mamatha, N.; Lingappa, B. A new approach to wood protection: Preliminary study of biologically synthesized copper oxide nanoparticle formulation as an environmental friendly wood protectant against decay fungi and termites. *Maderas. Ciencia y Tecnología* **2019**, *21*, 347–356. [CrossRef]
11. Lykidis, C.; De Troya, T.; Conde, M.; Galván, J.; Mantanis, G. Termite resistance of beech wood treated with zinc oxide and zinc borate nanocompounds. *Wood Mater. Sci. Eng.* **2018**, *13*, 45–49. [CrossRef]
12. Terzi, E.; Kartal, S.N.; Yılgör, N.; Rautkari, L.; Yoshimura, T. Role of various nano-particles in prevention of fungal decay, mold growth and termite attack in wood, and their effect on weathering properties and water repellency. *Int. Biodeterior. Biodegrad.* **2016**, *107*, 77–87. [CrossRef]
13. Mantanis, G.; Terzi, E.; Kartal, S.N.; Papadopoulos, A.N. Evaluation of mold, decay and termite resistance of pine wood treated with zinc- and copper-based nanocompounds. *Int. Biodeterior. Biodegrad.* **2014**, *90*, 140–144. [CrossRef]
14. Akhtari, M.; Nicholas, D. Evaluation of particulate zinc and copper as wood preservatives for termite control. *Eur. J. Wood Wood Prod.* **2013**, *71*, 395–396. [CrossRef]
15. Clausen, C.A.; Kartal, S.N.; Arango, R.A.; Green, F. The role of particle size of particulate nano-zinc oxide wood preservatives on termite mortality and leach resistance. *Nanoscale Res. Lett.* **2011**, *6*, 427. [CrossRef] [PubMed]
16. Dai, X.; Qi, Y.; Luo, H.; He, Z.; Wei, L.; Dong, X.; Ma, X.; Yang, D.-Q.; Li, Y. Leachability and anti-mold efficiency of nanosilver on poplar wood surface. *Polymers* **2022**, *14*, 884. [CrossRef] [PubMed]
17. Iqtedar, M.; Mirza, N.; Aihetasham, A.; Iftikhar, S.; Kaleem, A.; Abdullah, R. Termiticidal activity of mycosynthesized silver nanoparticles from *Aspergillus fumigatus* BTCB15. *Revista Mexicana de Ingeniería Química* **2020**, *19*, 1201–1211. [CrossRef]
18. Casado, S.; Silva, C.; Ponce, H.; Martín, R.; Martín, G.; Acuña, R. White-rot fungi control on populus spp. Wood by pressure treatments with silver nanoparticles, chitosan oligomers and propolis. *Forests* **2019**, *10*, 885. [CrossRef]
19. Silva-Castro, I.; Casados-Sanz, M.; Alonso-Cortés, A.; Martín-Ramos, P.; Martín-Gil, J.; Acuña-Rello, L. Chitosan-based coatings to prevent the decay of *Populus* spp. wood caused by *Trametes versicolor*. *Coatings* **2018**, *8*, 415. [CrossRef]
20. Moya, R.; Rodriguez-Zuñiga, A.; Berrocal, A.; Vega-Baudrit, J. Effect of silver nanoparticles synthesized with NPsAg-ethylene glycol ($C_2H_6O_2$) on brown decay and white decay fungi of nine tropical woods. *J. Nanosci. Nanotechnol.* **2017**, *17*, 5233–5240. [CrossRef]
21. Moya, R.; Berrocal Jiménez, A.; Rodríguez Zúñiga, A.; Vega Baudrit, J.; Chaves Noguera, S. Effect of silver nanoparticles on white-rot wood decay and some physical properties of three tropical wood species. *Wood Fiber Sci.* **2014**, *46*, 527–538.
22. Kartal, S.; Green, F.; Clausen, C. Do the unique properties of nanometals affect leachability or efficacy against fungi and termites? *Int. Biodeterior. Biodegrad.* **2009**, *63*, 490–495. [CrossRef]

23. Green, F.; Arango, R.A. Wood protection by commercial silver formulations against eastern subterranean termites. In Proceedings of the International Research Group on Wood Protection 38th Annual Meeting, Jackson Hole, WY, USA, 20–24 May 2007; p. 07-30422.

24. Dorau, B.; Arango, R.; Green, F. An investigation into the potential of ionic silver as a wood preservative. In Proceedings of the 2nd Woodframe Housing Durability and Disaster Issues Conference, Madison, WI, USA, 6–8 November 2004; pp. 133–145.

25. Yudaev, P.; Mezhuev, Y.; Chistyakov, E. Nanoparticle-containing wound dressing: Antimicrobial and healing effects. *Gels* **2022**, *8*, 329. [CrossRef]

26. Calovi, M.; Coroneo, V.; Rossi, S. Antibacterial efficiency over time and barrier properties of wood coatings with colloidal silver. *Appl. Microbiol. Biotechnol.* **2023**, *107*, 5975–5986. [CrossRef]

27. Piętka, J.; Adamczuk, A.; Zarzycka, E.; Tulik, M.; Studnicki, M.; Oszako, T.; Aleksandrowicz-Trzcińska, M. The application of copper and silver nanoparticles in the protection of *Fagus sylvatica* wood against decomposition by *Fomes fomentarius*. *Forests* **2022**, *13*, 1724. [CrossRef]

28. Aleksandrowicz-Trzcińska, M.; Szaniawski, A.; Olchowik, J.; Drozdowski, S. Effects of copper and silver nanoparticles on growth of selected species of pathogenic and wood-decay fungi in vitro. *For. Chron.* **2018**, *94*, 109–116. [CrossRef]

29. Bak, M.; Németh, R. Effect of different nanoparticle treatments on the decay resistance of wood. *BioResources* **2018**, *13*, 7886–7899. [CrossRef]

30. Pařil, P.; Baar, J.; Čermák, P.; Rademacher, P.; Prucek, R.; Sivera, M.; Panáček, A. Antifungal effects of copper and silver nanoparticles against white and brown-rot fungi. *J. Mater. Sci.* **2016**, *52*, 2720–2729. [CrossRef]

31. Arpanaei, A.; Fu, Q.; Singh, T. Nanotechnology approaches towards biodeterioration-resistant wood: A review. *J. Bioresour. Bioprod.* **2023**; *in press, corrected proof*. [CrossRef]

32. EPA. Overview of Wood Preservative Chemicals. Available online: https://www.epa.gov/ingredients-used-pesticide-products/overview-wood-preservative-chemicals (accessed on 16 November 2023).

33. Ali, S.; Chen, X.; Ahmad, S.; Shah, W.; Shafique, M.; Chaubey, P.; Mustafa, G.; Alrashidi, A.; Alharthi, S. Advancements and challenges in phytochemical-mediated silver nanoparticles for food packaging: Recent review (2021–2023). *Trends Food Sci. Technol.* **2023**, *141*, 104197. [CrossRef]

34. Mansoor, S.; Zahoor, I.; Baba, T.R.; Padder, S.A.; Bhat, Z.A.; Koul, A.M.; Jiang, L. Fabrication of silver nanoparticles against fungal pathogens. *Front. Nanotechnol.* **2021**, *3*, 679358. [CrossRef]

35. Silva-Castro, I.; Martín-García, J.; Diez, J.J.; Flores-Pacheco, J.A.; Martín-Gil, J.; Martín-Ramos, P. Potential control of forest diseases by solutions of chitosan oligomers, propolis and nanosilver. *Eur. J. Plant Pathol.* **2017**, *150*, 401–411. [CrossRef]

36. Matei, P.M.; Martín-Ramos, P.; Sánchez-Báscones, M.; Hernández-Navarro, S.; Correa-Guimaraes, A.; Navas-Gracia, L.M.; Rufino, C.A.; Ramos-Sánchez, M.C.; Martín-Gil, J. Synthesis of chitosan oligomers/propolis/silver nanoparticles composite systems and study of their activity against *Diplodia seriata*. *Int. J. Polym. Sci.* **2015**, *2015*, 864729. [CrossRef]

37. Woźniak, M.; Gromadzka, K.; Kwaśniewska-Sip, P.; Cofta, G.; Ratajczak, I. Chitosan–caffeine formulation as an ecological preservative in wood protection. *Wood Sci. Technol.* **2022**, *56*, 1851–1867. [CrossRef]

38. Mirda, E.; Idroes, R.; Khairan, K.; Tallei, T.E.; Ramli, M.; Earlia, N.; Maulana, A.; Idroes, G.M.; Muslem, M.; Jalil, Z. Synthesis of chitosan-silver nanoparticle composite spheres and their antimicrobial activities. *Polymers* **2021**, *13*, 3990. [CrossRef] [PubMed]

39. *UNE-EN 1995-1-1:2016*; Eurocode 5: Design of Timber Structures—Part 1-1: General—Common Rules and Rules for Buildings. Asociación Española de Normalización: Madrid, Spain, 2016.

40. Spavento, E.; Troya, M.T.; Casado-Sanz, M.; Santos, S.M.; Martín-Gil, J.; Martín-Ramos, P.; Robertson, L.; Acuña-Rello, L. Evaluation of the efficacy of silver nanoparticles and chitosan oligomer composites as poplar wood protective treatments against termites. In Proceedings of the IRG54 Annual Meeting, Cairns, Australia, 28 May–1 June 2023; p. IRG/WP 23-40963.

41. Bossert, D.; Geers, C.; Placencia Peña, M.I.; Volkmer, T.; Rothen-Rutishauser, B.; Petri-Fink, A. Size and surface charge dependent impregnation of nanoparticles in soft- and hardwood. *Chemistry* **2020**, *2*, 361–373. [CrossRef]

42. *EN 113-1:2021*; Durability of Wood and Wood-Based Products—Test Method against Wood Destroying Basidiomycetes—Part 1: Assessment of Biocidal Efficacy of Wood Preservatives. European Committee for Standardization: Brussels, Belgium, 2021; p. 31.

43. *EN 113-2:2021*; Durability of Wood and Wood-Based Products—Test Method against Wood Destroying Basidiomycetes—Part 2: Assessment of Inherent or Enhanced Durability. European Committee for Standardization: Brussels, Belgium, 2021; p. 29.

44. *EN 117:2012*; Wood Preservatives—Determination of Toxic Values against Reticulitermes Species (European Termites) (Laboratory Method). European Committee for Standardization: Brussels, Belgium, 2012; p. 22.

45. Buzón-Durán, L.; Martín-Gil, J.; Pérez-Lebeña, E.; Ruano-Rosa, D.; Revuelta, J.L.; Casanova-Gascón, J.; Ramos-Sánchez, M.C.; Martín-Ramos, P. Antifungal agents based on chitosan oligomers, ε-polylysine and *Streptomyces* spp. secondary metabolites against three *Botryosphaeriaceae* species. *Antibiotics* **2019**, *8*, 99. [CrossRef] [PubMed]

46. Ho, K.W.; Ooi, C.W.; Mwangi, W.W.; Leong, W.F.; Tey, B.T.; Chan, E.-S. Comparison of self-aggregated chitosan particles prepared with and without ultrasonication pretreatment as Pickering emulsifier. *Food Hydrocoll.* **2016**, *52*, 827–837. [CrossRef]

47. Santos-Moriano, P.; Fernandez-Arrojo, L.; Mengibar, M.; Belmonte-Reche, E.; Peñalver, P.; Acosta, F.N.; Ballesteros, A.O.; Morales, J.C.; Kidibule, P.; Fernandez-Lobato, M.; et al. Enzymatic production of fully deacetylated chitooligosaccharides and their neuroprotective and anti-inflammatory properties. *Biocatal. Biotransform.* **2018**, *36*, 57–67. [CrossRef]

48.   Arendrup, M.C.; Cuenca-Estrella, M.; Lass-Flörl, C.; Hope, W. EUCAST technical note on the EUCAST definitive document EDef 7.2: Method for the determination of broth dilution minimum inhibitory concentrations of antifungal agents for yeasts EDef 7.2 (EUCAST-AFST). *Clin. Microbiol. Infect.* **2012**, *18*, E246–E247. [CrossRef]

49.   Gokce, Y.; Cengiz, B.; Yildiz, N.; Calimli, A.; Aktas, Z. Ultrasonication of chitosan nanoparticle suspension: Influence on particle size. *Colloids Surf. A Physicochem. Eng. Asp.* **2014**, *462*, 75–81. [CrossRef]

50.   *EN 335:2013*; Durability of Wood and Wood-Based Products—Use Classes: Definitions, Application to Solid Wood and Wood-Based Products. European Committee for Standardization: Brussels, Belgium, 2013; p. 14.

51.   R Core Team. *R: A Language and Environment for Statistical Computing*; R Foundation for Statistical Computing: Vienna, Austria, 2022.

52.   Mikhailova, E.O. Silver nanoparticles: Mechanism of action and probable bio-application. *J. Funct. Biomater.* **2020**, *11*, 84. [CrossRef]

53.   Nel, A.; Xia, T.; Madler, L.; Li, N. Toxic potential of materials at the nanolevel. *Science* **2006**, *311*, 622–627. [CrossRef]

54.   Alghuthaymi, M.A.; Almoammar, H.; Rai, M.; Said-Galiev, E.; Abd-Elsalam, K.A. Myconanoparticles: Synthesis and their role in phytopathogens management. *Biotechnol. Biotechnol. Equip.* **2015**, *29*, 221–236. [CrossRef]

55.   Klaine, S.J.; Alvarez, P.J.J.; Batley, G.E.; Fernandes, T.F.; Handy, R.D.; Lyon, D.Y.; Mahendra, S.; McLaughlin, M.J.; Lead, J.R. Nanomaterials in the environment: Behavior, fate, bioavailability, and effects. *Environ. Toxicol. Chem.* **2009**, *27*, 1825–1851. [CrossRef] [PubMed]

56.   Jafernik, K.; Ładniak, A.; Blicharska, E.; Czarnek, K.; Ekiert, H.; Wiącek, A.E.; Szopa, A. Chitosan-based nanoparticles as effective drug delivery systems—A review. *Molecules* **2023**, *28*, 1963. [CrossRef] [PubMed]

57.   Can, A.; Sivrikaya, H.; Hazer, B.; Palanti, S. Beech (*Fagus orientalis*) wood modification through the incorporation of polystyrene-ricinoleic acid copolymer with Ag nanoparticles. *Cellulose* **2022**, *29*, 1149–1161. [CrossRef]

58.   Bugnicourt, L.; Alcouffe, P.; Ladavière, C. Elaboration of chitosan nanoparticles: Favorable impact of a mild thermal treatment to obtain finely divided, spherical, and colloidally stable objects. *Colloids Surf. A Physicochem. Eng. Asp.* **2014**, *457*, 476–486. [CrossRef]

59.   Babaee, M.; Garavand, F.; Rehman, A.; Jafarazadeh, S.; Amini, E.; Cacciotti, I. Biodegradability, physical, mechanical and antimicrobial attributes of starch nanocomposites containing chitosan nanoparticles. *Int. J. Biol. Macromol.* **2022**, *195*, 49–58. [CrossRef] [PubMed]

60.   Nascimento, T.; Rego, C.; Oliveira, H. Potential use of chitosan in the control of grapevine trunk diseases. *Phytopathologia Mediterranea* **2007**, *46*, 218–224.

61.   Venkatesham, M.; Ayodhya, D.; Madhusudhan, A.; Veera Babu, N.; Veerabhadram, G. A novel green one-step synthesis of silver nanoparticles using chitosan: Catalytic activity and antimicrobial studies. *Appl. Nanosci.* **2012**, *4*, 113–119. [CrossRef]

62.   Wang, L.-S.; Wang, C.-Y.; Yang, C.-H.; Hsieh, C.-L.; Chen, S.-Y.; Shen, C.-Y.; Wang, J.-J.; Huang, K.-S. Synthesis and anti-fungal effect of silver nanoparticles-chitosan composite particles. *Int. J. Nanomed.* **2015**, *10*, 2685. [CrossRef]

63.   Alfredsen, G.; Eikenes, M.; Militz, H.; Solheim, H. Screening of chitosan against wood-deteriorating fungi. *Scand. J. For. Res.* **2011**, *19*, 4–13. [CrossRef]

64.   Singh, T.; Vesentini, D.; Singh, A.P.; Daniel, G. Effect of chitosan on physiological, morphological, and ultrastructural characteristics of wood-degrading fungi. *Int. Biodeterior. Biodegrad.* **2008**, *62*, 116–124. [CrossRef]

65.   Torr, K.M.; Chittenden, C.; Franich, R.A.; Kreber, B. Advances in understanding bioactivity of chitosan and chitosan oligomers against selected wood-inhabiting fungi. *Holzforschung* **2005**, *59*, 559–567. [CrossRef]

66.   Guggiari, M.; Bloque, R.; Aragno, M.; Verrecchia, E.; Job, D.; Junier, P. Experimental calcium-oxalate crystal production and dissolution by selected wood-rot fungi. *Int. Biodeterior. Biodegrad.* **2011**, *65*, 803–809. [CrossRef]

67.   Rudakiya, D.M.; Gupte, A. Degradation of hardwoods by treatment of white rot fungi and its pyrolysis kinetics studies. *Int. Biodeterior. Biodegrad.* **2017**, *120*, 21–35. [CrossRef]

68.   Dutton, M.V.; Evans, C.S. Oxalate production by fungi: Its role in pathogenicity and ecology in the soil environment. *Can. J. Microbiol.* **1996**, *42*, 881–895. [CrossRef]

69.   Schwarze, F.W.M.R. Wood decay under the microscope. *Fungal Biol. Rev.* **2007**, *21*, 133–170. [CrossRef]